J Intell Robot Syst (2017) 85:127–144
DOI 10.1007/s10846-016-0378-4

Spatial Trajectory Tracking Control of a Fully Actuated Helicopter in Known Static Environment

Zhen Zhao · Wei He · Zhao Yin · Jun Zhang

Received: 21 March 2015 / Accepted: 2 May 2016 / Published online: 19 May 2016

Abstract In this paper, we consider the control problem of tracking a 3D spatial trajectory for a fully actuated helicopter in static known environment, which is predefined to avoid obstacles and collisions considering the distance, fuel consumption and other related constraints. For this purpose, a nonlinear controller using the radial basis function neural network (RBFNN) is designed. Based on Lyapunov analysis, the proposed adaptive neural network control succeeds in tracking the desired trajectory robustly to a small neighborhood of zero, and guarantees the boundedness of all the closed-loop signals at the same time. Extensive numerical results are given to illustrate the effectiveness of the designed controller.

Keywords Helicopter · Neural networks · Radial basis function · Adaptive control · Robot · Trajectory tracking

Z. Zhao
College of Electronic Information and Automation, Civil Aviation University of China, Tianjin 300300, China

W. He (✉)
School of Automation and Electrical Engineering, University of Science and Technology Beijing, Beijing 100083, China
e-mail: hewei.ac@gmail.com

Z. Yin
School of Automation Engineering, University of Electronic Science and Technology of China, Chengdu 611731, China

J. Zhang
College of Aerospace Engineering, Civil Aviation University of China, Tianjin 300300, China

1 Introduction

Aerial Vehicles (AVs) have been used more and more widely in surveillance, search and rescue mission, aerial mapping, cartography, border patrol, inspection, agricultural imaging, and other related areas [1–3]. During these flight missions, the AVs usually fly in low altitudes, which makes them be subject to collision with static obstacles (such as buildings, trees, mountains, etc.) as well as dynamic obstacles (such as other AVs, etc.) in their flight zone [1]. To avoid the potential collisions, static trajectories or real-time motion plans must be executed for the AVs in static environments or dynamic environments, respectively. After that, the AVs can be controlled to follow the desired trajectories or motion plans to avoid the potential collisions and achieve its goals [4].

This paper is concerned with the control problem of tracking a predefined 3D spatial trajectory in known static environment for a fully actuated helicopter, which means enabling the helicopter to move from its current location to a new desired location avoiding collisions with fixed obstacles. This control problem is challenging due to highly nonlinear and strongly coupled dynamics of the helicopter, such that disturbances along a single degree of freedom (DOF) can easily propagate to the other DOF and lead to loss of performance or even destabilization [5].

During the past few decades, flight control has attracted an ever increasing interest to guarantee the stability of helicopter systems. A large number of control techniques have been proposed in the literature for the flight control of helicopters, including sliding mode control [6], H_∞ control [7–10], backstepping control [11, 12], neural network control [13–15], and so on. In all of these flight control methods, model-based control, such as H_∞ control etc., is susceptible to uncertainties and disturbances. The authors proposed a robust attitude control of helicopters with actuator dynamics using neural networks to handle the model uncertainty and the external disturbance [15]. The authors developed an approximation-based techniques using neural networks (NN) to track the altitude and yaw angle for a scale model helicopter mounted on an experimental platform in the presence of model uncertainties [5]. Both of these controllers were designed to track the states of the helicopter with limited flight zone. The authors proposed a robust full degree of freedom tracking control to follow the vertical, lateral, longitudinal and yaw attitude motion of a helicopter along the desired arbitrary trajectories [16]. However, they have simplified the vector of forces applied to the helicopter.

The neural network and adaptive control is designed to track the planned trajectory that is very common in many areas. For example, robotic system, marine system and other nonlinear system [17–30]. In [31], the authors addressed the problem of control design for strict-feedback systems with constraints on the states via neural network. The authors presented the neural network control for a rehabilitation robot with unknown system dynamics in [32]. For the marine system, the authors investigated the control problem of tracking a desired trajectory by adaptive neural network [33]. An adaptive output feedback control was studied for uncertain nonlinear systems with unmeasured states in [34]. The authors proposed an online learning adaptive neural network for small unmanned aerial vehicle (UAV) to improve control performance during flight [35]. The authors investigated a novel method to solve the mutual synchronization control problem of multiple robot manipulators in the case that the desired trajectory is only available to a portion of the team members, and the dynamics and the external disturbances of the manipulators are unknown in [36]. The representative works on mobile manipulators are [37–41]. In these papers [37–39, 41], some elegant techniques for mobile manipulators, such as operation space transformation, hybrid force/motion, symmetrical and asymmetrical coordination, can be employed to give rise to the performance of mobile manipulators, evenly other robots, which were significant improvement in robotic applications. In addition, fuzzy logic control [42–53] is also widely used for the nonlinear systems and their applications with uncertainties.

In this paper, we draw inspiration from the attitude and yaw angle tracking for a scale model helicopter mounted on an experimental platform in the presence of nonlinearity, model uncertainty and external disturbance. The approximated-based NN control is designed to track the desired 3D spatial trajectory. RBFNN realizes function approximation through mapping input-output as a linear combination of radially symmetric functions [54]. Compared with other neural network structure, RBFNN illustrates good properties, such as rapid training, good generalization, simplicity structure, etc.. For this reason, this article chooses RBFNN in our controller. The main contributions of this paper include:

(i) An implementable robust and adaptive RBFNN controller is designed to track the planned 3D spatial trajectory in known static environment.
(ii) Virtual control input is introduced during the control design process to make the system stable.
(iii) Uniform boundedness and stability are proved via Lyapunov synthesis.

The rest of this paper is organized as follows. Section 2 illustrates the dynamics of the fully actuated helicopter and some preliminaries. In Section 3, the adaptive RBFNN control design via Lyapunov's method is discussed for autonomous tracking the desired 3D trajectory. The numerical simulation is presented in Section 4 to verify performance of the proposed controller. The conclusion of this paper is drawn in Section 5.

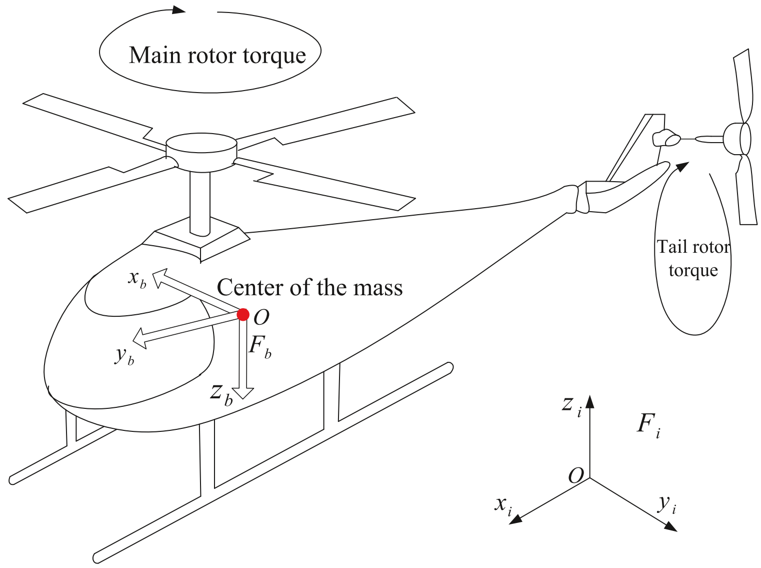

Fig. 1 A helicopter system

2 Problem Formulation and Preliminaries

In the following study, the notations and definitions are used throughout the whole paper. $\Re^n$ denotes the n-dimensional Euclidean space. $\Re^+$ represents the positive real number.

Assumption 1 *The planned 3D spatial trajectories* $[x_{1d}(t), x_{2d}(t), x_{3d}(t)]^T$ *and their derivatives up to the third order are continuously differentiable and bounded for all* $t \geq 0$.

2.1 Dynamic Analysis

As shown in Fig. 1, by fixing an inertial coordinate frame F_i in the Euclidean space and a reference coordinate frame F_b attached to the body of the helicopter, a mathematical model of the helicopter dynamics can be derived from Newton-Euler equations of motion of a rigid body in the inertial coordinate frame. The multiple-input-multiple-output (MIMO) non-linear model of a six degree-of-freedom (DOF$_6$) helicopter is described as below [8, 16, 55]:

$$\begin{aligned} M\ddot{p} &= Rf^b, \\ J\dot{\omega} &= -S(\omega)J\omega + \tau^b. \end{aligned} \tag{1}$$

where $p = [p_x, p_y, p_z]^T$ represents the position of the center of the mass; $\omega = [\omega_1, \omega_2, \omega_3]^T$ denotes the angular velocities along the x, y and z axes; M is the mass of the body; J is the inertia tensor of the body which is a diagonal matrix; f^b and τ^b are the vector of forces and torques in the body-fixed coordinate system; R is a rotation matrix, and $S(\omega)$ denotes the 3×3 skew-symmetric matrix, shown as Eq. 2.

$$\begin{aligned} R &= \begin{bmatrix} 1 & \sin\phi\tan\theta & \cos\phi\tan\theta \\ 0 & \cos\phi & -\sin\phi \\ 0 & \sin\phi/\cos\theta & \cos\phi/\cos\theta \end{bmatrix}, \\ S(\omega) &= \begin{bmatrix} 0 & -\omega_3 & \omega_2 \\ \omega_3 & 0 & -\omega_1 \\ -\omega_2 & \omega_1 & 0 \end{bmatrix}. \end{aligned} \tag{2}$$

The expressions of f^b and τ^b are in terms of four control inputs $u = [P_M, P_T, \alpha, \beta]^T$, where P_M and P_T represent the main rotor collective pitch and the tail rotor collective pitch, α and β denote the longitudinal and lateral inclination of the tip path plane in the body-fixed coordinate system. From previous work of Isidori et al. [56], Koo and Sastry [57] and Marconi [16], f^b and τ^b can be modeled as:

$$\begin{aligned} f^b &= \begin{bmatrix} X_M & Y_M + Y_T & Z_M \end{bmatrix}^T + R^T \begin{bmatrix} 0 & 0 & Mg \end{bmatrix}^T, \\ \tau^b &= \begin{bmatrix} R_M \\ M_M \\ N_M \end{bmatrix} + \begin{bmatrix} Y_M h_m + Z_M y_m + Y_T h_t \\ -X_M h_m + Z_M l_m \\ -Y_M l_m - Y_T l_t \end{bmatrix}. \end{aligned} \tag{3}$$

where g is the force of gravity; l_m, y_m, h_m and l_t, y_t, h_t represent the coordinates of the main and tail rotor shafts with respect to the center of the mass in F_b; $X_M = -T_M \sin\alpha$, $Y_M = T_M \sin\beta$, $Z_M = -T_M \cos\alpha\cos\beta$, $Y_T = -T_T$, $R_M = c_b^M \beta - Q_M \sin\alpha$, $M_M = c_a^M \alpha + Q_M \sin\beta$ and $N_M = -Q_M \cos\alpha\cos\beta$.

In these expressions, c_a^M and c_b^M are physical parameters modeling the flapping dynamic of the main rotor, Q_M is the total torque of the main rotor, T_M and T_T are the thrusts generated by the main and tail rotor respectively, which are given by:

$$T_M = K_{T_M}\omega_e^2 P_M, \tag{4}$$
$$T_T = K_{T_T}\omega_e^2 P_T. \tag{5}$$

where ω_e is the angular velocity of the main rotor in F_b, K_{T_M} and K_{T_T} denote aerodynamic constants of the main and tail rotors' blades. ω_e is dominated by the engine dynamic model, which is modeled as [58]

$$Q_e = P_e/\omega_e, \qquad P_e = \bar{P}_e T_h. \tag{6}$$

where Q_e is the total engine torques, and P_e denotes engine power which is assumed to be proportional to throttle T_h with $0 < T_h < 1$.

Let $x_1 = p_x, x_2 = p_y, x_3 = p_z, x_4 = \omega_1, x_5 = \omega_2, x_6 = \omega_3, u_1 = P_M, u_2 = P_T, u_3 = \alpha$ and $u_4 = \beta$. At the mean time, considering that the tilt angles α and β are small, we have $\sin\alpha \approx \alpha$, $\sin\beta \approx \beta$, $\cos\alpha \approx 1$ and $\cos\beta \approx 1$. Substitute Eqs. 2, 3, 4 and 5 into Eq. 1, we have the following helicopter system:

$$A(x)\ddot{x} + B(x,\dot{x})\dot{x} + C(x) = D(x,u) \tag{7}$$

where $x, \dot{x}, \ddot{x}$ represent the state vector, first order differential state vector, and second order differential state vector, respectively. The matrix coefficients are given as follows:

$$A(x) = \begin{bmatrix} l_m M & 0 & 0 & 0\ 0\ 0 \\ 0 & l_m M & 0 & 0\ 0\ 0 \\ 0 & M\frac{\sin\phi}{\cos\theta} & -M\cos\phi & 0\ 0\ 0 \\ 0 & 0 & 0 & 0\ 0\ 0 \\ 0 & 0 & 0 & 0\ 0\ 0 \\ 0 & 0 & 0 & 0\ 0\ 0 \end{bmatrix}_{6\times 6}$$

$$B(x,\dot{x}) = -\begin{bmatrix} 0\ 0\ 0 & 0 & 0 & -J_{33}\sin\phi\tan\theta \\ 0\ 0\ 0 & 0 & 0 & -J_{33}\cos\phi \\ 0\ 0\ 0 & 0 & 0 & 0 \\ 0\ 0\ 0 & J_{11} & 0 & 0 \\ 0\ 0\ 0 & 0 & J_{22} & 0 \\ 0\ 0\ 0 & 0 & 0 & J_{33} \end{bmatrix}_{6\times 6},$$

$$C(x) = -\begin{bmatrix} (J_{11}-J_{22})x_4x_5\sin\phi\tan\theta + l_m M g\frac{\tan\theta}{\cos\theta} \\ (J_{11}-J_{22})\cos\phi x_4x_5 - Q_M\cos\phi \\ -Mg\frac{\cos\phi}{\cos^2\theta} \\ (J_{22}-J_{33}x_5x_6) \\ (J_{33}-J_{11})x_4x_6 \\ (J_{11}-J_{22})x_4x_5 - Q_M \end{bmatrix}_{6\times 1},$$

$$\begin{aligned} D(x,u) &= \begin{bmatrix} -l_m K_{T_M}\omega_e^2\cos\phi\tan\theta\cdot u_1 + (l_t-l_m)K_{T_T}\omega_e^2\sin\phi\tan\theta\cdot u_2 - l_m K_{T_M}\omega_e^2\cdot u_1u_3 \\ l_m K_{T_M}\omega_e^2\sin\phi\cdot u_1 + (l_t-l_m)K_{T_T}\omega_e^2\cdot u_2 \\ \frac{K_{T_M}\omega_e^2}{\cos\theta}\cdot u_1 \\ -y_m K_{T_M}\omega_e^2\cdot u_1 - h_t K_{T_T}\omega_e^2\cdot u_2 - Q_M\cdot u_3 + (h_m K_{T_M}\omega_e^2\cdot u_1 + c_b^M)\cdot u_4 \\ -l_m K_{T_M}\omega_e^2\cdot u_1 + h_m K_{T_M}\omega_e^2\cdot u_1u_3 + c_a^M u_3 + Q_M\cdot u_4 \\ -l_m K_{T_M}\omega_e^2\cdot u_1u_4 + l_t K_{T_T}\omega_e^2\cdot u_2 \end{bmatrix}_{6\times 1} \\ &= \begin{bmatrix} d_{11} & d_{12} & d_{13}(u_1) & 0 \\ d_{21} & d_{22} & 0 & 0 \\ d_{31} & 0 & 0 & 0 \\ d_{41} & d_{42} & d_{43} & d_{44}(u_1) \\ d_{51} & 0 & d_{53}(u_1) & d_{54} \\ 0 & d_{62} & 0 & d_{64}(u_1) \end{bmatrix} \times \begin{bmatrix} u_1 \\ u_2 \\ u_3 \\ u_4 \end{bmatrix}. \end{aligned} \tag{8}$$

The control objective is to track an 3D planned trajectory of helicopter in known environment. Therefore, the proposed control techniques must render the helicopter track a desired trajectory $[x_{1d}, x_{2d}, x_{3d}]^T$ such that the tracking errors converge to a very small neighborhood of the desired position, that is, $\lim_{t\to t_i} \|[x_1(t), x_2(t), x_3(t)]^T - [x_{1d}(t_i), x_{2d}(t_i), x_{3d}(t_i)]^T\| < \epsilon$ with $\epsilon > 0$ ensuring that the helicopter would not collide with other obstacles.

Assumption 2 [15, 59] *For all $t > 0$, there exist $\|\dot{x}_{id}(t)\| \le \zeta_{1i}$, $\|\ddot{x}_{id}(t)\| \le \zeta_{2i}$ and $\|x_{id}^{(3)}(t)\| \le \zeta_{3i}$ ($i = 1, 2, 3$), where $\zeta_{1i} > 0$, $\zeta_{2i} > 0$ and $\zeta_{3i} > 0$.*

2.2 Preliminaries

Assumption 3 [5] *On a compact set* $\Omega_Z \subset \Re^{n+1}$*, the ideal neural network weights* W^* *satisfy*

$$\|W^*\| \leq w_m \tag{9}$$

where w_m *is a positive constant.*

Lemma 1 [60–62] *For bounded initial conditions, if there exists a* C^1 *continuous and positive definite Lyapunov function* $V(x)$ *satisfying* $\gamma_1(\|x\|) \leq V(x) \leq \gamma_2(\|x\|)$*, such that* $\dot{V}(x) \leq -\rho V(x) + \eta$*, where* $\gamma_1, \gamma_2 : \Re^n \rightarrow \Re$ *are class K functions,* ρ *and* η *are positive constants, then the solution* $x(t)$ *is uniformly bounded.*

Lemma 2 *For* $a, b \in \Re^+$*, the following inequality holds:*

$$\frac{ab}{a+b} \leq a \tag{10}$$

3 Spatial Trajectory Tracking Controller Design

The main control purpose is to design the four control inputs $u = [P_M, P_T, \alpha, \beta]^T$ in order to asymptotically track the planned 3D spatial trajectory $[x_{1d}(t), x_{2d}(t), x_{3d}(t)]^T$. The planned 3D spatial trajectory of each helicopter can be calculated by optimizing an objective function, for example, distance and fuel consumption, with constraints corresponding to some special airspace traffic rules. In this paper, the planned 3D spatial trajectory from the trajectory planning method is assumed to be known. Motivated by the the previous work on the approximated-based control of helicopter [5], we will design adaptive neural control for each subsystem to follow the planned 3D spatial trajectory.

3.1 RBFNN-based control

In this section, the RBFNN-based controller designed by Lyapunov synthesis is developed to track the planned trajectory. From Eq. 7, we have six subsystems in sequence. With respect to the obtained six subsystems, the controller is designed step by step as follows:

1) Design u_1 based on the 3^{rd} subsystem;
2) Design u_2 based on the 2^{nd} subsystem;
3) Design u_3 based on the 1^{st} subsystem;
4) Design u_4 based on the 4^{th} subsystem;
5) Analyze the stability of internal dynamics of 5^{th} and 6^{th} subsystem.

3.1.1 3^{rd} Subsystem

From Eq. 7, we have the 3^{rd} subsystem as:

$$a_{32}\ddot{x}_2 + a_{33}\ddot{x}_3 + c_3 = d_{31}u_1 \tag{11}$$

Define a new virtual state variable $x_{new} = a_{32}x_2 + a_{33}x_3$, then the tracking error and filtered tracking error can be defined as below:

$$e_{new} = x_{new} - x_{newd}, \tag{12}$$

$$r_{new} = \dot{e}_{new} + \lambda_3 e_{new} \tag{13}$$

where $x_{newd} = a_{32}x_{2d} + a_{33}x_{3d}$, λ_3 is a designed positive real constant.

Substituting Eqs. 12, 13 into Eq. 11, we have

$$\dot{r}_{new} = d_{31}u_1 - F_{S1} \tag{14}$$

where

$$F_{S1} = \ddot{x}_{newd} - \lambda_3\dot{e}_{new} + c_3 \tag{15}$$

is an unknown nonlinear function, which can be approximated by a RBFNN to arbitrary any accuracy as

$$F_{S1} = W_1^{*T} S_1(Z_1) + \varepsilon_1(Z_1) \tag{16}$$

where $Z_1 = [\ddot{x}_{newd}, \dot{e}_{new}]^T \in \Omega_{Z_1}$ is the input vector of the NN; $S_1(Z_1)$ is the basis function; W_1^* is ideal weight satisfying $\|W_1^*\| \leq \omega_{1m}$, where ω_{1m} is a positive constant; $\varepsilon_1(Z_1)$ is the approximation error satisfying $\varepsilon_1(Z_1) \leq \bar{\varepsilon}_1$, where $\bar{\varepsilon}_1$ is a positive constant.

Let $\hat{W}_1$ approximates W_1^*, then the error between the actual and the ideal RBFNN is as below:

$$\hat{W}_1^T S_1(Z_1) - W_1^{*T} S_1(Z_1) = \tilde{W}_1^T S_1(Z_1) \tag{17}$$

where $\tilde{W}_1 = \hat{W}_1 - W_1^*$.

Consider the following Lyapunov function candidate

$$V_1 = \frac{1}{2}r_{new}^2 + \frac{1}{2}\tilde{W}_1^T \Gamma_1^{-1} \tilde{W}_1 \tag{18}$$

where $\Gamma_1 = \Gamma_1^T > 0$.

The time derivative of V_1 is given by

$$\begin{aligned}\dot{V}_1 &= r_{new}\dot{r}_{new} + \tilde{W}_1^T\Gamma_1^{-1}\dot{\tilde{W}}_1\\ &= r_{new}[d_{31}u_1 - W_1^{*T}S_1(Z_1) - \varepsilon_1(Z_1)] + \tilde{W}_1^T\Gamma_1^{-1}\dot{\hat{W}}_1\end{aligned} \tag{19}$$

Consider the following RBFNN based control law and weight adaptation law

$$u_1 = -k_1 r_{new} - \frac{r_{new}(\hat{W}_1^T S_1(Z_1))^2}{d_{31}(|r_{new}\hat{W}_1^T S_1(Z_1)| + \delta_1)}, \tag{20}$$

$$\dot{\hat{W}}_1 = -\Gamma_1[S_1(Z_1)r_{new} + \sigma_1\hat{W}_1]. \tag{21}$$

where $k_1 > 0$, $\delta_1 > 0$, and $\sigma_1 > 0$.

Remark 1 The above σ-modification adaptation term $\sigma_1\hat{W}_1$ in Eq. 21 is introduced to improve the robustness in the presence of the RBFNN approximation error ε_1 [63–66]. Furthermore, $\sigma_1\hat{W}_1$ can easily be replaced by e-modification adaptation term like $\sigma_1|r_{new}|\hat{W}_1$. In this way, the control design in this paper can be easily extended to the control based on e-modification adaptation law without difficulty.

Substituting Eqs. 17, 20 and 21 into Eq. 19, we have

$$\begin{aligned}\dot{V}_1 &= -k_1 d_{31}{r_{new}}^2 - \frac{{r_{new}}^2(\hat{W}_1^T S_1(Z_1))^2}{|r_{new}\hat{W}_1^T S_1(Z_1)| + \delta_1}\\ &\quad -r_{new}W_1^{*T}S_1(Z_1) - r_{new}\varepsilon_1(Z_1)\\ &\quad -r_{new}\tilde{W}_1^T S_1(Z_1) - \sigma_1\tilde{W}_1^T\hat{W}_1\\ &\le -k_1 d_{31}{r_{new}}^2 - \frac{{r_{new}}^2(\hat{W}_1^T S_1(Z_1))^2}{|r_{new}\hat{W}_1^T S_1(Z_1)| + \delta_1}\\ &\quad +|r_{new}\hat{W}_1^T S_1(Z_1)|\\ &\quad +|r_{new}||\varepsilon_1(Z_1)| - \sigma_1\tilde{W}_1^T\hat{W}_1\end{aligned} \tag{22}$$

Noting that

$$\begin{aligned}&-\frac{{r_{new}}^2(\hat{W}_1^T S_1(Z_1))^2}{|r_{new}\hat{W}_1^T S_1(Z_1)| + \delta_1} + |r_{new}\hat{W}_1^T S_1(Z_1)|\\ &= \frac{|r_{new}\hat{W}_1^T S_1(Z_1)|\delta_1}{|r_{new}\hat{W}_1^T S_1(Z_1)| + \delta_1}.\end{aligned} \tag{23}$$

According to Lemma 2, Eq. 23 yields

$$-\frac{{r_{new}}^2(\hat{W}_1^T S_1(Z_1))^2}{|r_{new}\hat{W}_1^T S_1(Z_1)| + \delta_1} + |r_{new}\hat{W}_1^T S_1(Z_1)| \le \delta_1. \tag{24}$$

By completion of squares, we can obtain

$$\begin{aligned}-\sigma_1\tilde{W}_1^T\hat{W}_1 &= -\sigma_1\tilde{W}_1^T(\tilde{W}_1 + W_1^*)\\ &\le -\frac{\sigma_1}{2}\|\tilde{W}_1\|^2 + \frac{\sigma_1}{2}\|W_1^*\|^2.\end{aligned} \tag{25}$$

According to the Young's inequality, we have

$$|r_{new}||\varepsilon_1(Z_1)| \le \frac{r_{new}^2}{2\theta_1} + \frac{\theta_1\varepsilon_1^2}{2} \le \frac{r_{new}^2}{2\theta_1} + \frac{\theta_1\bar{\varepsilon}_1^2}{2}. \tag{26}$$

where $\theta_1 > 0$.

Substituting Eqs. 24–26, we have

$$\begin{aligned}\dot{V}_1 &\le -(k_1 d_{31} - \frac{1}{2\theta_1})r_{new}^2 - \frac{\sigma_1}{2}\|\tilde{W}_1\|^2 + \delta_1\\ &\quad +\frac{\theta_1}{2}\bar{\varepsilon}_1^2 + \frac{\sigma_1}{2}\omega_{1m}^2\\ &\le -\frac{1}{2}(2k_1 d_{31} - 1/\theta_1)r_{new}^2\\ &\quad -\frac{1}{2}\frac{\sigma_1}{\lambda_{\max}(\Gamma_1^{-1})}\tilde{W}_1^T\Gamma_1^{-1}\tilde{W}_1 + \delta_1\\ &\quad +\frac{\theta_1}{2}\bar{\varepsilon}_1^2 + \frac{\sigma_1}{2}\omega_{1m}^2\\ &\le -\min\left\{2k_1 d_{31} - 1/\theta_1, \frac{\sigma_1}{\lambda_{\max}(\Gamma_1^{-1})}\right\}\\ &\quad \times\left[\frac{1}{2}r_{new}^2 + \frac{1}{2}\tilde{W}_1^T\Gamma_1^{-1}\tilde{W}_1\right] + \delta_1 + \frac{\theta_1}{2}\bar{\varepsilon}_1^2\\ &\quad +\frac{\sigma_1}{2}\omega_{1m}^2\\ &\le -\rho_{10}V_1 + \eta_{10}.\end{aligned} \tag{27}$$

where $\lambda_{\max}(\cdot)$ denotes the largest eigenvalue of a matrix; $\rho_{10} = \min\left\{2k_1 d_{31} - 1/\theta_1, \frac{\sigma_1}{\lambda_{\max}(\Gamma_1^{-1})}\right\}$, $\eta_{10} = \delta_1 + \frac{\theta_1}{2}\bar{\varepsilon}_1^2 + \frac{\sigma_1}{2}\omega_{1m}^2$.

3.1.2 2^{nd} Subsystem

From Eq. 7, we have the 2^{nd} subsystem as below:

$$a_{22}\ddot{x}_2 + b_2(x,\dot{x})\dot{x}_6 + c_2(x) = d_{21}u_1 + d_{22}u_2 \tag{28}$$

Similar to Section 3.1.1, define the tracking error and filtered tracking error as below:

$$e_2 = x_2 - x_{2d}, \tag{29}$$

$$r_2 = \dot{e}_2 + \lambda_2 e_2 \tag{30}$$

where λ_2 is a designed positive real constant.

Substituting Eqs. 29, 30 into x_2 subsystem, we have

$$a_{22}\dot{r}_2 = d_{22}u_2 - F_{S2}. \tag{31}$$

where

$F_{S2} = a_{22}(\ddot{x}_{2d} - \lambda_2 \dot{e}_2) + b_2(x, \dot{x})\dot{x}_6 + c_2(x) - d_{21}u_1$

is an unknown nonlinear function, which is approximated by RBFNN to arbitrary any accuracy as

$$F_{S2} = {W_2^*}^T S_2(Z_2) + \varepsilon_2(Z_2) \tag{32}$$

where $Z_2 = [x_4 x_5, \dot{x}_6, \dot{e}_2, \ddot{x}_{2d}, u_1]^T \in \Omega_{Z_2}$ is the input vector of the NN; $S_2(Z_2)$ is the basis function; W_2^* is ideal weight satisfying $\|W_2^*\| \le \omega_{2m}$, where ω_{2m} is a positive constant; $\varepsilon_2(Z_2)$ is the approximation error satisfying $\varepsilon_2(Z_2) \le \bar{\varepsilon}_2$, where $\bar{\varepsilon}_2$ is a positive constant.

Let $\hat{W}_2$ approximate W_2^*, then the error between the actual and the ideal RBFNN can be expressed as below:

$$\hat{W}_2^T S_2(Z_2) - {W_2^*}^T S_2(Z_2) = \tilde{W}_2^T S_2(Z_1) \tag{33}$$

where $\tilde{W}_2 = \hat{W}_2 - W_2^*$.

Consider the following Lyapunov function candidate

$$V_1 = \frac{1}{2}a_{22}r_2^2 + \frac{1}{2}\tilde{W}_2^T \Gamma_2^{-1}\tilde{W}_2 \tag{34}$$

where $\Gamma_2 = \Gamma_2^T > 0$.

The time derivative of V_2 is given by

$$\begin{aligned} \dot{V}_2 &= a_{22}r_2\dot{r}_2 + \tilde{W}_2^T \Gamma_2^{-1}\dot{\hat{W}}_2 \\ &= r_2\left[d_{22}u_2 - {W_2^*}^T S_2(Z_2) - \varepsilon_2(Z_2)\right] \\ &\quad + \tilde{W}_2^T \Gamma_2^{-1}\dot{\hat{W}}_2 \end{aligned} \tag{35}$$

Consider the following NN based control law and weight adaptation law

$$u_2 = -k_2 r_2 - \frac{r_2(\hat{W}_2^T S_2(Z_2))^2}{d_{22}(|r_2\hat{W}_2^T S_2(Z_2)| + \delta_2)}, \tag{36}$$

$$\dot{\hat{W}}_2 = -\Gamma_2\left[S_2(Z_2)r_2 + \sigma_2\hat{W}_2\right]. \tag{37}$$

where $k_2 > 0$, $\delta_2 > 0$, and $\sigma_2 > 0$.

Substituting Eqs. 33, 36 and 37 into Eq. 35, we have

$$\begin{aligned} \dot{V}_2 &= -k_2 d_{22}{r_2}^2 - \frac{{r_2}^2(\hat{W}_2^T S_2(Z_2))^2}{|r_2\hat{W}_2^T S_2(Z_2)| + \delta_2} \\ &\quad - r_2{W_2^*}^T S_2(Z_2) - r_2\varepsilon_2(Z_2) - r_2\tilde{W}_2^T S_2(Z_2) \\ &\quad - \sigma_2\tilde{W}_2^T\hat{W}_2 \\ &\le -k_2 d_{22}{r_2}^2 - \frac{{r_2}^2(\hat{W}_2^T S_2(Z_2))^2}{|r_2\hat{W}_2^T S_2(Z_2)| + \delta_2} \\ &\quad + |r_2\hat{W}_2^T S_2(Z_2)| + |r_2||\varepsilon_2(Z_2)| - \sigma_2\tilde{W}_2^T\hat{W}_2. \end{aligned} \tag{38}$$

Similar to Eqs. 24, 25 and 26, the following inequalities hold

$$-\frac{{r_2}^2(\hat{W}_2^T S_2(Z_2))^2}{|r_2\hat{W}_2^T S_2(Z_2)| + \delta_2} + |r_2\hat{W}_2^T S_2(Z_2)| \le \delta_2 \tag{39}$$

$$-\sigma_2\tilde{W}_1^T\hat{W}_1 \le -\frac{\sigma_2}{2}\|\tilde{W}_2\|^2 + \frac{\sigma_2}{2}\|W_2^*\|^2. \tag{40}$$

$$|r_2||\varepsilon_2(Z_2)| \le \frac{r_2^2}{2\theta_2} + \frac{\theta_2\bar{\varepsilon}_2^2}{2}. \tag{41}$$

where $\theta_2 > 0$.

Substituting Eqs. 39–41 into Eq. 38, we have

$$\begin{aligned} \dot{V}_2 &\le -(k_2 d_{22} - \frac{1}{\theta_2})r_2^2 - \frac{\sigma_2}{2}\|\tilde{W}_2\|^2 + \delta_2 \\ &\quad + \frac{\theta_2}{2}\bar{\varepsilon}_2^2 + \frac{\sigma_2}{2}\omega_{2m}^2 \\ &\le -\frac{1}{2}a_{22}\frac{2k_2 d_{22} - 1/\theta_2}{a_{22}}r_2^2 \\ &\quad - \frac{1}{2}\frac{\sigma_2}{\lambda_{\max}(\Gamma_2^{-1})}\tilde{W}_2^T\Gamma_2^{-1}\tilde{W}_2 + \delta_2 \\ &\quad + \frac{\theta_2}{2}\bar{\varepsilon}_2^2 + \frac{\sigma_2}{2}\omega_{2m}^2 \\ &\le -\min\left\{\frac{2k_2 d_{22} - 1/\theta_2}{a_{22}}, \frac{\sigma_2}{\lambda_{\max}(\Gamma_2^{-1})}\right\} \\ &\quad \times \left[\frac{1}{2}a_{22}r_2^2 + \frac{1}{2}\tilde{W}_2^T\Gamma_2^{-1}\tilde{W}_2\right] + \delta_2 \\ &\quad + \frac{\theta_2}{2}\bar{\varepsilon}_2^2 + \frac{\sigma_2}{2}\omega_{2m}^2 \\ &\le -\rho_{20}V_2 + \eta_{10}. \end{aligned} \tag{42}$$

where $\rho_{20} = \min\left\{\frac{2k_2 d_{22} - 1/\theta_2}{a_{22}}, \frac{\sigma_2}{\lambda_{\max}(\Gamma_2^{-1})}\right\}$, $\eta_{20} = \delta_2 + \frac{\theta_2}{2}\bar{\varepsilon}_2^2 + \frac{\sigma_2}{2}\omega_{2m}^2$.

3.1.3 1^{st} Subsystem

From Eq. 7, we have the 1^{st} subsystem as below:

$$\begin{aligned} a_{11}\ddot{x}_1 + b_{16}\dot{x}_6 + c_1(x) &= d_{11}u_1 + d_{12}u_2 \\ &\quad + l_m K_{T_M}\omega_e^2 u_1 u_3 \end{aligned} \tag{43}$$

Similar to Section 3.1.2, define the tracking error and filtered tracking error as below:

$$e_1 = x_1 - x_{1d}, \tag{44}$$

$$r_1 = \dot{e}_1 + \lambda_1 e_1 \tag{45}$$

where λ_1 is a designed positive real constant.

Similar to Sections 3.1.1 and 3.1.2, substituting Eqs. 44, 45 into x_1 subsystem, we have

$$a_{11}\dot{r}_1 = d_{13}u_1u_3 - F_{S3} \tag{46}$$

where

$$F_{S3} = a_{11}(\ddot{x}_{1d} - \lambda_1\dot{e}_1) + b_{16}\dot{x}_6 + c_1(x) - d_{11}u_1 - d_{12}u_2$$

is an unknown nonlinear function, which is approximated by RBFNN to arbitrary any accuracy as

$$F_{S3} = {W_3^*}^T S_3(Z_3) + \varepsilon_3(Z_3) \tag{47}$$

where $Z_3 = [x_4x_5, \dot{e}_1, \ddot{x}_{1d}, \dot{x}_6, u_1, u_2]^T \in \Omega_{Z_3}$ is the input vector of the RBFNN; $S_3(Z_3)$ is the basis functions; W_3^* is ideal weight satisfying $\|W_3^*\| \leq \omega_{3m}$, where ω_{3m} is a positive constant; $\varepsilon_3(Z_3)$ is the approximation error satisfying $\varepsilon_3(Z_3) \leq \bar{\varepsilon}_3$, where $\bar{\varepsilon}_3$ is a positive constant.

Let $\hat{W}_3$ approximate W_3^*, then the error between the actual and the ideal RBFNN can be expressed as below:

$$\hat{W}_3^T S_3(Z_3) - {W_3^*}^T S_3(Z_3) = \tilde{W}_3^T S_3(Z_3) \tag{48}$$

where $\tilde{W}_3 = \hat{W}_3 - W_3^*$.

Consider the following Lyapunov function candidate

$$V_3 = \frac{1}{2}a_{11}r_1^2 + \frac{1}{2}\tilde{W}_3^T\Gamma_3^{-1}\tilde{W}_3 \tag{49}$$

where $\Gamma_3 = \Gamma_3^T > 0$.

The time derivative of V_3 is given by

$$\begin{aligned}\dot{V}_3 &= a_{11}r_1\dot{r}_1 + \tilde{W}_3^T\Gamma_3^{-1}\dot{\hat{W}}_3 \\ &= r_1\left[d_{13}u_1u_3 - {W_3^*}^T S_3(Z_3) - \varepsilon_3(Z_3)\right] \\ &\quad + \tilde{W}_3^T\Gamma_3^{-1}\dot{\hat{W}}_3\end{aligned} \tag{50}$$

Suppose that $u_3' = u_1u_3$ is a virtual control input. Then, consider the following RBFNN based control law and weight adaptation law

$$u_3' = -k_3r_1 - \frac{r_1(\hat{W}_3^T S_3(Z_3))^2}{d_{13}(|r_1\hat{W}_3^T S_3(Z_3)| + \delta_3)}, \tag{51}$$

$$\dot{\hat{W}}_3 = -\Gamma_3\left[S_3(Z_3)r_1 + \sigma_3\hat{W}_3\right] \tag{52}$$

where $k_3 > 0$, $\delta_3 > 0$, $\underline{d}_{13}$ is a positive real constant such that $0 < \underline{d}_{13} \leq |d_{13}(u_1)|$, and $\sigma_3 > 0$.

Furthermore, the real control input u_3 can be defined as

$$u_3 = \begin{cases} u_3', & \text{if } u_1 = 0 \\ \frac{u_3'}{u_1}, & \text{Otherwise} \end{cases} \tag{53}$$

Substituting Eqs. 48, 51 and 52 into Eq. 50, we have

$$\begin{aligned}\dot{V}_3 &= -k_3d_{13}{r_1}^2 - \frac{{r_1}^2(\hat{W}_3^T S_3(Z_3))^2}{|r_1\hat{W}_3^T S_3(Z_3)| + \delta_3} \\ &\quad - r_1{W_3^*}^T S_3(Z_3) - r_1\varepsilon_3(Z_3) \\ &\quad - r_1\tilde{W}_3^T S_3(Z_3) - \sigma_3\tilde{W}_3^T\hat{W}_3 \\ &\leq -k_3d_{13}{r_1}^2 - \frac{{r_1}^2(\hat{W}_3^T S_3(Z_3))^2}{|r_1\hat{W}_3^T S_3(Z_3)| + \delta_3} \\ &\quad + |r_1\hat{W}_3^T S_3(Z_3)| + |r_1||\varepsilon_3(Z_3)| - \\ &\quad \sigma_3\tilde{W}_3^T\hat{W}_3\end{aligned} \tag{54}$$

Similar to Eqs. 24, 25 and 26, the following inequalities hold

$$-\frac{{r_1}^2(\hat{W}_3^T S_3(Z_3))^2}{|r_1\hat{W}_3^T S_3(Z_3)| + \delta_3} + |r_1\hat{W}_3^T S_3(Z_3)| \leq \delta_3 \tag{55}$$

$$-\sigma_3\tilde{W}_3^T\hat{W}_3 \leq -\frac{\sigma_3}{2}\|\tilde{W}_3\|^2 + \frac{\sigma_3}{2}\|W_3^*\|^2. \tag{56}$$

$$|r_1||\varepsilon_3(Z_3)| \leq \frac{r_1^2}{2\theta_3} + \frac{\theta_3\bar{\varepsilon}_3^2}{2}. \tag{57}$$

where $\theta_3 > 0$.

Substituting Eqs. 55–57, we have

$$\begin{aligned}\dot{V}_3 &\leq -(k_3d_{13} - \frac{1}{2\theta_3})r_1^2 - \frac{\sigma_3}{2}\|\tilde{W}_3\|^2 + \delta_3 \\ &\quad + \frac{\theta_3}{2}\bar{\varepsilon}_3^2 + \frac{\sigma_3}{2}\omega_{3m}^2 \\ &\leq -\frac{1}{2}a_{11}\frac{2k_3d_{13} - 1/\theta_3}{a_{11}}r_1^2 \\ &\quad - \frac{1}{2}\frac{\sigma_3}{\lambda_{\max}(\Gamma_3^{-1})}\tilde{W}_3^T\Gamma_3^{-1}\tilde{W}_3 + \delta_3 \\ &\quad + \frac{\theta_3}{2}\bar{\varepsilon}_3^2 + \frac{\sigma_3}{2}\omega_{3m}^2 \\ &\leq -\min\left\{\frac{2k_3d_{13} - 1/\theta_3}{a_{11}}, \frac{\sigma_3}{\lambda_{\max}(\Gamma_3^{-1})}\right\} \\ &\quad \times\left[\frac{1}{2}a_{11}r_1^2 + \frac{1}{2}\tilde{W}_3^T\Gamma_3^{-1}\tilde{W}_3\right] + \delta_3 \\ &\quad + \frac{\theta_3}{2}\bar{\varepsilon}_3^2 + \frac{\sigma_3}{2}\omega_{3m}^2 \\ &\leq -\rho_{30}V_3 + \eta_{30}.\end{aligned} \tag{58}$$

where $\rho_{30} = \min\left\{\frac{2k_3 d_{13} - 1/\theta_3}{a_{11}}, \frac{\sigma_3}{\lambda_{\max}(\Gamma_3^{-1})}\right\}$, $\eta_{30} = \delta_3 + \frac{\theta_3}{2}\bar{\varepsilon}_3^2 + \frac{\sigma_3}{2}\omega_{3m}^2$.

3.1.4 4^{th} Subsystem

From Eq. 7, we have the 4^{th} subsystem as below:

$$b_{44}\dot{x}_4 + c_4(x) = d_{41}u_1 + d_{42}u_2 + d_{43}u_3 + (h_m K_{T_M}\omega_e^2 u_1 + C_b^M)u_4 \quad (59)$$

To design u_4, we define an error variable $e_4 = x_4 - \tau$, where $\tau \in \Re$ is a virtual control law. Differentiating e_4 with respect to time yields

$$\dot{e}_4 = \dot{x}_4 - \dot{\tau}. \quad (60)$$

The virtual control law τ is chosen as

$$\tau = b_{44}(-k_\tau e_1 + x_{1d}). \quad (61)$$

where $k_\tau > 0$.

Substituting Eq. 60 into Eq. 59, we have

$$b_{44}\dot{e}_4 = d_{44}(u_1)u_4 - F_{S4}. \quad (62)$$

where

$$F_{S4} = b_{44}\dot{\tau} + c_4(x) - d_{41}u_1 - d_{42}u_2 - d_{43}u_3$$

is an unknown nonlinear function, which is approximated by RBFNN to arbitrary any accuracy as

$$F_{S4} = W_4^{*T} S_4(Z_4) + \varepsilon_4(Z_4) \quad (63)$$

where $Z_4 = [x_5 x_6, \dot{\tau}, u_1, u_2, u_3]^T \in \Omega_{Z_4}$ is the input vector of the RBFNN; $S_4(Z_4)$ are the basis functions; W_4^* are ideal weights satisfying $\|W_4^*\| \leq \omega_{4m}$, where ω_{4m} is a positive constant; $\varepsilon_4(Z_4)$ is the approximation error satisfying $\varepsilon_4(Z_4) \leq \bar{\varepsilon}_4$, where $\bar{\varepsilon}_4$ is a positive constant.

Let $\hat{W}_4$ approximate W_4^*, then the error between the actual and the ideal RBFNN can be expressed as below:

$$\hat{W}_4^T S_4(Z_4) - W_4^{*T} S_4(Z_4) = \tilde{W}_4^T S_4(Z_4) \quad (64)$$

where $\tilde{W}_4 = \hat{W}_4 - W_4^*$.

Consider the following Lyapunov function candidate

$$V_4 = V_3 + \frac{1}{2}b_{44}e_4^2 + \frac{1}{2}\tilde{W}_4^T\Gamma_4^{-1}\tilde{W}_4 \quad (65)$$

where $\Gamma_4 = \Gamma_4^T > 0$.

The time derivative of V_4 is given by

$$\begin{aligned} \dot{V}_4 &= \dot{V}_3 + b_{44}e_4\dot{e}_4 + \tilde{W}_4^T\Gamma_4^{-1}\dot{\hat{W}}_4 \\ &= \dot{V}_3 + e_4\Big[(h_m K_{T_M}\omega_e^2 u_1 + C_b^M)u_4 \\ &\quad - W_4^{*T} S_4(Z_4) - \varepsilon_4(Z_4)\Big] + \tilde{W}_4^T\Gamma_4^{-1}\dot{\hat{W}}_4 \end{aligned} \quad (66)$$

Choose $(h_m K_{T_M}\omega_e^2 u_1 + C_b^M)u_4$ as a new virtual control input u_4', and consider the following RBFNN based control law and weight adaptation law

$$u_4' = -k_4 e_4 - \frac{e_4(\hat{W}_4^T S_4(Z_4))^2}{(|e_4\hat{W}_4^T S_4(Z_4)| + \delta_4)}, \quad (67)$$

$$\dot{\hat{W}}_4 = -\Gamma_4\Big[S_4(Z_4)e_4 + \sigma_4\hat{W}_4\Big]. \quad (68)$$

where $k_4 > 0$, $\delta_4 > 0$, $\underline{d}_{44}$ is a positive constant such that $0 < \underline{d}_{44} \leq |d_{44}(u_1)|$, and $\sigma_4 > 0$.

For the real control input u_4, it can be defined as

$$u_4 = \begin{cases} u_4', & \text{if } h_m K_{T_M}\omega_e^2 u_1 + C_b^M = 0 \\ \frac{u_4'}{h_m K_{T_M}\omega_e^2 u_1 + C_b^M}, & \text{Otherwise} \end{cases} \quad (69)$$

Substituting Eqs. 64, 67 and 68 into Eq. 66, we have

$$\begin{aligned} \dot{V}_4 &= \dot{V}_3 + e_4\left[-k_4 e_4 - \frac{(\hat{W}_4^T S_4(Z_4))^2}{(|e_4\hat{W}_4^T S_4(Z_4)| + \delta_4)}\right] \\ &\quad - e_4 W_4^{*T} S_4(Z_4) - e_4\varepsilon_4(Z_4) \\ &\quad - \tilde{W}_4^T\Big[S_4(Z_4)e_4 - \sigma_4\hat{W}_4\Big] \\ &\leq \dot{V}_3 - k_4 {e_4}^2 - \frac{e_4^2(\hat{W}_4^T S_4(Z_4))^2}{|e_4\hat{W}_4^T S_4(Z_4)| + \delta_4} \\ &\quad + |e_4\hat{W}_4^T S_4(Z_4)| + |e_4||\varepsilon_4(Z_4)| \\ &\quad - \sigma_4\tilde{W}_4^T\hat{W}_4. \end{aligned} \quad (70)$$

Similar to Eqs. 24, 25 and 26, the following inequalities hold

$$-\frac{{e_4}^2(\hat{W}_4^T S_4(Z_4))^2}{|e_4\hat{W}_4^T S_4(Z_4)| + \delta_4} + |e_4\hat{W}_4^T S_4(Z_4)| \leq \delta_4 \quad (71)$$

$$-\sigma_4\tilde{W}_4^T\hat{W}_4 \leq -\frac{\sigma_4}{2}\|\tilde{W}_4\|^2 + \frac{\sigma_4}{2}\|W_4^*\|^2. \quad (72)$$

$$|e_4||\varepsilon_4(Z_4)| \leq \frac{e_4^2}{2\theta_4} + \frac{\theta_4\bar{\varepsilon}_4^2}{2}. \quad (73)$$

where $\theta_4 > 0$.

Substituting Eqs. 71-73, we have

$$\begin{aligned}\dot{V}_4 \leq & -\min\left\{\frac{2k_3d_{13}-\frac{1}{\theta_3}}{a_{11}}, \frac{\sigma_3}{\lambda_{\max}(\Gamma_3^{-1})}, \frac{2k_4-\frac{1}{\theta_4}}{b_{44}}, \frac{\sigma_4}{\lambda_{\max}(\Gamma_4^{-1})}\right\} \\ & \times\left[(\frac{1}{2}a_{11}r_1^2+\frac{1}{2}\tilde{W}_3^T\Gamma_3^{-1}\tilde{W}_3) \right. \\ & \left. +(\frac{1}{2}b_{44}e_4^2+\frac{1}{2}\tilde{W}_4^T\Gamma_4^{-1}\tilde{W}_4)\right]+\eta_{30}+\delta_4+\frac{\theta_4}{2}\bar{\varepsilon}_4^2+\frac{\sigma_4}{2}\omega_{4m}^2 \\ \leq & -\rho_{40}V_4+\eta_{40}. \end{aligned} \tag{74}$$

where $\rho_{40} = \min\left\{\frac{2k_3d_{13}-1/\theta_3}{a_{11}}, \frac{\sigma_3}{\lambda_{\max}(\Gamma_3^{-1})}, \frac{2k_4-1/\theta_4}{b_{44}}, \frac{\sigma_4}{\lambda_{\max}(\Gamma_4^{-1})}\right\}$, $\eta_{40} = \eta_{30}+\delta_4+\frac{\theta_4}{2}\bar{\varepsilon}_4^2+\frac{\sigma_4}{2}\omega_{4m}^2$.

3.1.5 5^{th} Subsystem

Using the designed control laws expressed by Eqs. 20, 36, 51 and 67, the 5^{th} subsystem can be written as

$$\dot{\xi} = \psi(\varrho, \xi, \upsilon). \tag{75}$$

where $\xi = x_5$, $\varrho = [x_4, x_6]^T$, $\upsilon = [u_1, u_3, u_4]^T$.

The zero-dynamics can be addressed as [5]

$$\dot{\xi} = \psi(0, \xi, \upsilon^*(0, \xi)) \tag{76}$$

Assumption 4 [5] *System (7) is hyperbolically minimum-phase. As such, zero-dynamics (76) is exponentially stable. Furthermore, noting that the control input υ is a function of (ξ, ϱ) and the reference signal satisfying Assumption 2, the function $\psi(\xi, \varrho, \upsilon)$ is Lipschitz in ϱ, i.e. there exist constants L_ϱ and L_ψ for $\psi(\xi, \varrho, \upsilon)$ such that*

$$\|\psi(\xi, \varrho, \upsilon) - \psi(0, \xi, \upsilon_\xi)\| \leq L_\varrho\|\varrho\| + L_\psi \tag{77}$$

where $\upsilon_\xi = \upsilon^*(0, \xi)$.

According to Assumption 4 and the Converse Theorem of Lyapunov [5], there exists a Lyapunov function $V_5(\xi)$ which satisfies

$$\gamma_a\|\xi\|^2 \leq V_5(\xi) \leq \gamma_b\|\xi\|^2 \tag{78}$$

$$\frac{\partial V_5}{\partial \xi}\psi(0, \xi, \tau_\xi) \leq -\nu_a\|\xi\|^2 \tag{79}$$

$$\left\|\frac{\partial V_5}{\partial \xi}\right\| \leq \nu_b\|\xi\| \tag{80}$$

where γ_a, γ_b, ν_a and ν_b are positive constants.

Lemma 3 [5] *For the internal dynamics $\dot{\xi} = \psi(\varrho, \xi, \upsilon)$ of the system, if Assumption 4 is satisfied, and the states ϱ are bounded by a positive constant $\|\varrho\|_{\max}$, i.e. $\|\varrho\| \leq \|\varrho\|_{\max}$, then there exist positive constants L_ξ and T_0 such that*

$$\|\xi(t)\| \leq L_\eta,\ \forall t > T_0 \tag{81}$$

Proof According to Assumption 4, there exists a Lyapunov function $V_5(\xi)$. Differentiating $V_5(\xi)$, we have

$$\begin{aligned}\dot{V}_5(\xi) &= \frac{\partial V_0}{\partial \xi}\dot{\xi} = \frac{\partial V_5}{\partial \xi}\psi(\varrho, \xi, \upsilon) \\ &= \frac{\partial V_5}{\partial \xi}\psi(0, \xi, \upsilon_\xi) \\ &\quad + \frac{\partial V_5}{\partial \xi}[\psi(\varrho, \xi, \upsilon) - \psi(0, \xi, \upsilon_\xi)]\end{aligned} \tag{82}$$

Noting that Eqs. 77–80, 82 can be written as

$$\begin{aligned}\dot{V}_5(\xi) &\leq -\nu_a\|\xi\|^2 + \nu_b\|\xi\|(L_\varrho\|\varrho\| + L_\psi) \\ &\leq -\nu_a\|\xi\|^2 + \nu_b\|\xi\|(L_\varrho\|\varrho\|_{\max} + L_\psi)\end{aligned}$$

Therefore, $\dot{V}_5(\xi) \leq 0$ whenever

$$\|\xi\| \geq \frac{\nu_b}{\nu_a}(L_\varrho\|\varrho\|_{\max} + L_\psi)$$

Let $L_\xi = \nu_b/(r\nu_a)(L_\varrho\|\varrho\|_{\max}+L_\psi)$, it can be concluded that there exists a positive constant T_0, such that Eq. 81 holds. □

3.1.6 6^{th} Subsystem

Similar to Section 3.1.5, the 6^{th} subsystem can be written as

$$\dot{\xi}' = \varphi(\varrho', \xi', \upsilon') \tag{83}$$

where $\xi' = x_6$, $\varrho' = [x_4, x_5]^T$, $\upsilon' = [u_1, u_2, u_4]^T$.

The zero-dynamics is as below:

$$\dot{\xi}' = \varphi(0, \xi', \upsilon'^*(0, \xi')) \tag{84}$$

Similar to Assumption 4, there exist constant $L_{\varrho'}$ and $L_{\varphi'}$ such that

$$\|\varphi(\xi', \varrho', \upsilon') - \varphi(0, \xi', \upsilon'_{\xi'})\| \leq L_{\varrho'}\|\varrho'\| + L_{\varphi'} \tag{85}$$

where $\upsilon'_{\xi'} = \upsilon'^*(0, \xi')$.

Furthermore, according to Assumption 4 and the Converse Theorem of Lyapunov [5], there exists a Lyapunov function $V_6(\xi')$ which satisfies

$$\gamma_a'\|\xi'\|^2 \leq V_6(\xi') \leq \gamma_b'\|\xi'\|^2 \tag{86}$$

$$\frac{\partial V_6}{\partial \xi'}\varphi(0,\xi',\upsilon_{\xi'}') \leq -\nu_a'\|\xi'\|^2 \tag{87}$$

$$\|\frac{\partial V_6}{\partial \xi'}\| \leq \nu_b'\|\xi'\| \tag{88}$$

where γ_a', γ_b', ν_a' and ν_b' are positive constants.

Lemma 4 [5] *For the internal dynamics $\dot{\xi}' = \varphi(\varrho',\xi',\upsilon')$ of the system, if Assumption 4 is satisfied, and the states ϱ' are bounded by a positive constant $\|\varrho'\|_{\max}$, i.e. $\|\varrho'\| \leq \|\varrho'\|_{\max}$, then there exist positive constants $L_{\xi'}$ and T_0' such that*

$$\|\xi'(t)\| \leq L_{\xi'},\ \forall t > T_0' \tag{89}$$

Proof The proof of Lemma 4 is the same to that of Lemma 3. It is omitted here for clarity and conciseness. □

3.2 Stability Analysis

The following theorem shows the stability and control performance of the control system.

Theorem 1 *Consider the system (7), the control laws (20), (36), (51), (67) and the adaptive laws (21), (37), (52), (68). Under Assumptions 2–4, the overall closed-loop adaptive neural network control system is SGUUB in the sense that all of the variables in the system are bounded, the tracking errors and neural weights converge to the following regions*

$$\begin{aligned}
|e_1| &\leq |e_1(0)| + \frac{1}{\lambda_1}\sqrt{\frac{2\eta_3}{d_{11}}} \\
|e_2| &\leq |e_2(0)| + \frac{1}{\lambda_2}\sqrt{\frac{2\eta_2}{d_{21}}} \\
|e_3| &\leq |e_3(0)| + \frac{1}{\lambda_3}\sqrt{\frac{2\eta_1}{d_{31}}} \\
\|\hat{W}_1\| &\leq \sqrt{\frac{2\eta_1}{\lambda_{\min}(\Gamma_1^{-1})}} + \omega_{1m} \\
\|\hat{W}_2\| &\leq \sqrt{\frac{2\eta_2}{\lambda_{\min}(\Gamma_2^{-1})}} + \omega_{2m} \\
\|\hat{W}_3\| &\leq \sqrt{\frac{2\eta_3}{\lambda_{\min}(\Gamma_3^{-1})}} + \omega_{3m} \\
\|\hat{W}_4\| &\leq \sqrt{\frac{2\eta_4}{\lambda_{\min}(\Gamma_4^{-1})}} + \omega_{4m}.
\end{aligned} \tag{90}$$

where

$$\eta_i = \frac{\eta_{i0}}{\rho_{i0}} + V_i(0),\ \ \eta_{i0} = \delta_i + \frac{1}{2}\bar{\varepsilon}_i^2 + \frac{\sigma_i}{2}\omega_{im}^2,\ i = 1,2,3,4$$

$$\rho_{10} = \min\left\{\frac{2k_1b_{31} - 1/c_1}{d_{31}}, \frac{\sigma_1}{\lambda_{\max}(\Gamma_1^{-1})}\right\}$$

$$\rho_{20} = \min\left\{\frac{2k_2b_{22} - 1/c_2}{d_{21}}, \frac{\sigma_2}{\lambda_{\max}(\Gamma_2^{-1})}\right\}$$

$$\rho_{30} = \min\left\{\frac{2k_3\underline{b}_{13} - 1/c_3}{d_{11}}, \frac{\sigma_3}{\lambda_{\max}(\Gamma_3^{-1})}\right\}$$

$$\rho_{40} = -\min\left\{\frac{2k_3\underline{b}_{13} - 1/c_3}{d_{11}}, \frac{\sigma_3}{\lambda_{\max}(\Gamma_3^{-1})}, \frac{2k_4\underline{b}_{42} - 1/c_4}{d_{41}}, \frac{\sigma_4}{\lambda_{\max}(\Gamma_4^{-1})}\right\}$$

$e_i(0) (i = 1,2,3)$ and $V_i(0) (i = 1,2,3,4)$ are respectively the initial values of $e_i(t)$ and $V_i(t)$.

Proof From previous analysis, the closed-loop stability analysis of the 3^{rd} subsystem (11) with the control law u_1 (20) and the adaptive law (21) is made by

Table 1 Parameters of the helicopter system

Parameter	Value	Unit
J	diag(0.18,0.34,0.28)	Kg m^2
l_m	0	m
y_m	0	m
h_m	0.24	m
l_t	0.9	m
h_t	0.1	m
$c_M^{Q,T}$	52	N·m/rad
$c_{a,b}^M$	52	N·m/rad
K_{T_M}	58	mN·s^2/rad^3
K_{T_T}	1	mN·s^2/rad^3
M	8	Kg
$\bar{P}_e$	2000	W
T_h	0.2	mN·m/rad^2
ω_e	16	rad/s

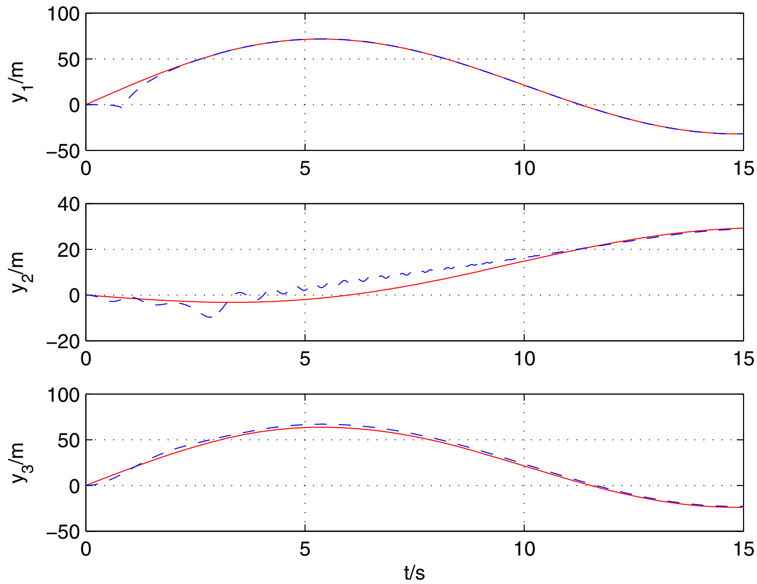

Fig. 2 Comparison between the desired trajectory and the simulated trajectory (solid line-the desired trajectory, dash line-the simulated trajectory)

Lyapunov synthesis. Then, similar closed-loop stability will be achieved on the subsystems (28), (43) and (59) with the control laws (36), (51), (67) and the adaptive laws (37), (52), (68). At last, the stability analysis of internal dynamics of the 5^{th} and 6^{th} subsystems are made based on the stability of the previous four subsystems.

The 3^{rd} *subsystem* Solving the inequality (27), we have $0 \leq V_1(t) \leq \eta_1$ with $\eta_1 = (\eta_{10}/\rho_{10}) + V_1(0)$.

Then, from the definition of $V_1(t)$ (18), we have

$$|r_3| \leq \sqrt{\frac{2\eta_1}{d_{31}}}, \ \|\tilde{W}_1\| \leq \sqrt{\frac{2\eta_1}{\lambda_{\min}(\Gamma_1^{-1})}} \tag{91}$$

From Eq. 13, we have $\dot{e}_{new} = -\lambda_3 e_{new} + r_{new}$. Thus, e_{new} can be solved as the following:

$$e_{new} = e^{-\lambda_3 t} e_{new}(0) + \int_0^t e^{-\lambda_3(t-\tau)} r_{new} d\tau \tag{92}$$

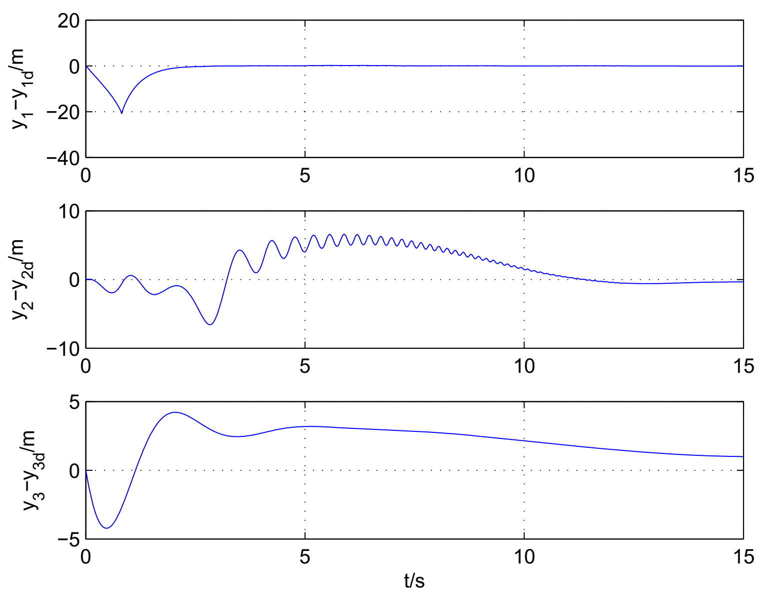

Fig. 3 Absolute error between the desired trajectory and the simulated trajectory

Combining Eqs. 91 and 92, we obtain

$$|e_{new}| \leq |e_{new}(0)| + \frac{1}{\lambda_3}\sqrt{\frac{2\eta_1}{d_{31}}} \tag{93}$$

Noting $x_{new} = e_{new} + x_{newd}$, $\hat{W}_1 = \tilde{W}_1 + W_1^*$, $\|W_1^*\| \leq \omega_{1m}$, and Assumption 2, we have

$$|x_{new}| \leq |e_{new}| + |x_{newd}| \leq |e_{new}(0)| + \frac{1}{\lambda_3}\sqrt{\frac{2\eta_1}{d_{31}}} + |x_{3d}| \in L_\infty$$

$$\|\hat{W}_1\| \leq \|\tilde{W}_1\| + \|W_1^*\| \leq \sqrt{\frac{2\eta_1}{\lambda_{\min}(\Gamma_1^{-1})}} + \omega_{1m} \in L_\infty.$$

Since the control law u_1 is a function of r_3 and $\hat{W}_1$, its boundedness is also guaranteed.

The 2^{nd} subsystem Similar to the stability analysis of the 3^{rd} subsystem, we have

$$|r_2| \leq \sqrt{\frac{2\eta_2}{d_{21}}}, \ \|\tilde{W}_2\| \leq \sqrt{\frac{2\eta_2}{\lambda_{\min}(\Gamma_2^{-1})}}$$

$$|e_2| \leq |e_2(0)| + \frac{1}{\lambda_2}\sqrt{\frac{2\eta_2}{d_{21}}}$$

$$|x_2| \leq |e_2| + |x_{2d}| \leq |e_2(0)| + \frac{1}{\lambda_2}\sqrt{\frac{2\eta_2}{d_{21}}} + |x_{2d}| \in L_\infty$$

$$\|\hat{W}_2\| \leq \|\tilde{W}_2\| + \|W_2^*\| \leq \sqrt{\frac{2\eta_2}{\lambda_{\min}(\Gamma_2^{-1})}} + \omega_{2m} \in L_\infty$$

and thus the boundedness of the control law u_2 is guaranteed.

The 1^{st} subsystem Similar to the stability analysis of the 3^{rd} and 2^{nd} subsystems, we have

$$|r_1| \leq \sqrt{\frac{2\eta_3}{d_{11}}}, \ \|\tilde{W}_3\| \leq \sqrt{\frac{2\eta_3}{\lambda_{\min}(\Gamma_3^{-1})}}$$

$$|e_1| \leq |e_1(0)| + \frac{1}{\lambda_1}\sqrt{\frac{2\eta_3}{d_{11}}}$$

$$|x_1| \leq |e_1| + |x_{1d}| \leq |e_1(0)| + \frac{1}{\lambda_1}\sqrt{\frac{2\eta_3}{d_{11}}} + |x_{1d}| \in L_\infty$$

$$\|\hat{W}_3\| \leq \|\tilde{W}_3\| + \|W_3^*\| \leq \sqrt{\frac{2\eta_3}{\lambda_{\min}(\Gamma_3^{-1})}} + \omega_{3m} \in L_\infty$$

and thus the boundedness of the control law u_3 is guaranteed.

The 4^{th} subsystem Solve the inequality (74), we have $0 \leq V_4(t) \leq \eta_4$ with $\eta_4 = (\eta_{40}/\rho_{40}) + V_4(0)$. According to the definition of V_4 (65), the following inequalities hold

$$|e_4| \leq \sqrt{\frac{2\eta_4}{d_{41}}}, \ \|\tilde{W}_4\| \leq \sqrt{\frac{2\eta_4}{\lambda_{\min}(\Gamma_4^{-1})}} \tag{94}$$

Fig. 4 Norm of neural weights using RBFNN-based control

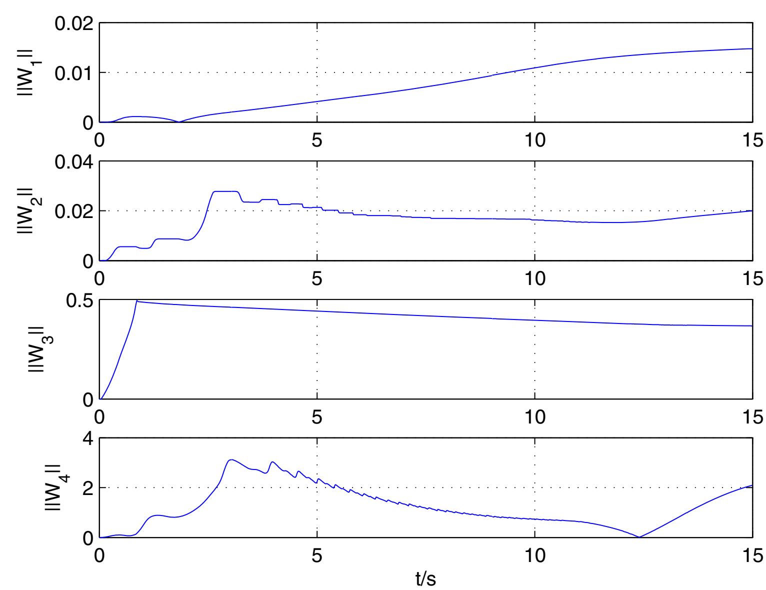

From Eq. 61, the virtual control law is bounded as the following

$$\begin{aligned}|\tau| &\leq |d_{41}k_\tau||e_1| + |x_{1d}| \\ &\leq |d_{41}k_\tau|\left(|e_1(0)| + \frac{1}{\lambda_1}\sqrt{\frac{2\eta_3}{d_{11}}}\right) + |x_{1d}|. \end{aligned} \tag{95}$$

Noting that $x_4 = e_4 + \tau$, $\hat{W}_4 = \tilde{W}_4 + W_4^*$, $\|W_4^*\| \leq \omega_{4m}$, and Assumption 2, we obtain

$$\begin{aligned}|x_4| &\leq |e_4| + |\tau| \leq \sqrt{\frac{2\eta_4}{d_{41}}} \\ &\quad +|d_{41}k_\tau|\left(|e_1(0)| + \frac{1}{\lambda_1}\sqrt{\frac{2\eta_3}{d_{11}}}\right) \\ &\quad +|x_{1d}| \in L_\infty \\ &\quad \|\hat{W}_4\| \leq \|\tilde{W}_4\| + \|W_4^*\| \\ &\leq \sqrt{\frac{2\eta_4}{\lambda_{\min}(\Gamma_4^{-1})}} + \omega_{4m} \in L_\infty \end{aligned}$$

The 5^{th} and 6^{th} subsystems From the previous stability analysis about the 1^{st}-4^{th} subsystems, it can be found that $x_1, x_2, x_3, x_4, \dot{x}_1, \dot{x}_2, \dot{x}_3, \dot{x}_4$ are all bounded. According to Lemma 3, we know that the internal dynamics is stable, i.e. x_5, x_6, $\dot{x}_5$ and $\dot{x}_6$ are also bounded. All the variables in the closed-loop system are bounded. □

4 Numerical Simulation

In this section, numerical simulations are given to demonstrate the feasibility and effectiveness of the proposed 3D spatial trajectory tracking control techniques. We choose the desired trajectories as follows: $y_d(t) = [y_1(t), y_2(t), y_3(t)]$, where

$$\begin{cases} y_1(t) = 30\sin(\pi t/40) + 60\sin(\pi t/10); \\ y_2(t) = 21\sin(\pi t/40) - 10\sin(\pi t/10); \\ y_3(t) = 30\sin(\pi t/40) + 52\sin(\pi t/10); \end{cases} \tag{96}$$

Detailed parameters of the helicopter system [16] are given in Table 1:

The control parameters for the RBFNN control laws (20), (36), (53), (69) and adaptation laws (21), (37), (52), (68) are chosen as follows: $k_1 = 2.925 \times 10^{-4}$, $\delta_1 = 1 \times 10^{-10}$, $\Gamma_1 = 3.165 \times 10^{-5}$, $\sigma_1 = 0.5$, $\lambda_1 = 2.5$, $k_2 = 0.5 \times 10^{-5}$, $\delta_2 = 1 \times 10^{-10}$, $\Gamma_2 = 6 \times 10^{-3}$, $\sigma_2 = 0.8$, $\lambda_2 = 2$, $k_3 = 1.2 \times 10^{-6}$, $\delta_3 = 1 \times 10^{-10}$, $\Gamma_3 = 1.5 \times 10^{-2}$, $\sigma_3 = 1.4$, $\lambda_3 = 2.893$, $k_4 = 1.01 \times 10^{-4}$, $\delta_4 = 1 \times 10^{-10}$, $\Gamma_4 = 3.4 \times 10^{-1}$, $\sigma_4 = 1.8$, and $k_\tau = 1.05$.

Figure 2 shows the comparison between the desired trajectory and the actual trajectory, from which, it can be seen that the actual trajectory can track the desired trajectory successfully along the x and z axes, the actual trajectory track the desired trajectory with fairly great error at the beginning along the y axis, but finally approaches to very small error. In

Fig. 5 Control inputs

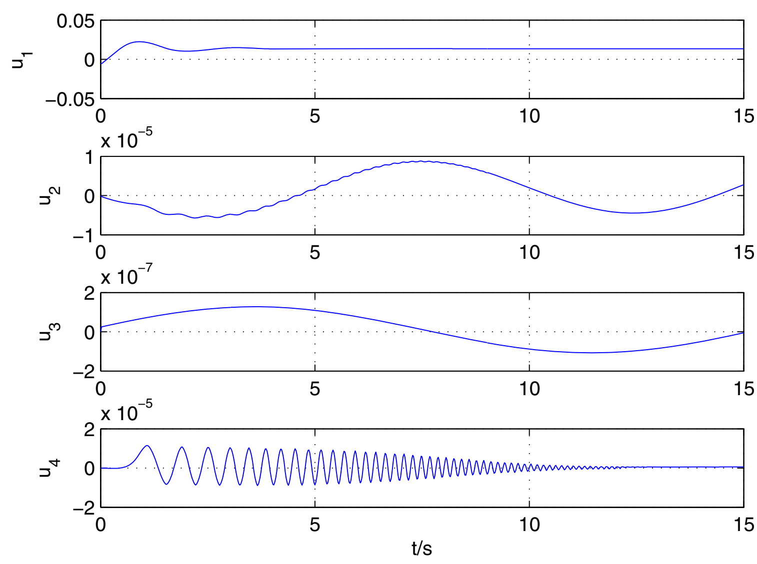

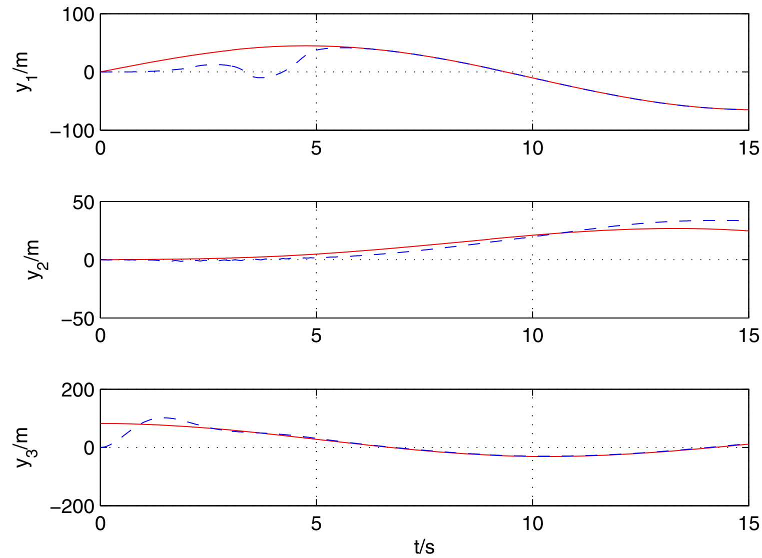

Fig. 6 Comparison between the desired trajectory and the simulated trajectory with different scenario (solid line-the desired trajectory, dash line-the simulated trajectory)

summary, the trajectory following ability in the 3D space is acceptable.

Figure 3 shows the tracking errors along the x, y and z axes. From Fig. 3, we can obtain the tracking errors converge to a relative small neighborhood after a short time about 12s using the RBFNN-based control method. The oscillations during the beginning 12s may be induced by the uncertainty learning process of RBFNN. After this oscillation period, the robustness to uncertainties is improved and the good tracking performance is achieved.

Figure 4 shows the corresponding norm of neural weights, and the control inputs are proposed by Fig. 5. From these two figures, we can see that both the norm of neural weights and the four control inputs are all bounded. From this perspective, the proposed RBFNN-based tracking control method for a fully actuated helicopter in known static environment is feasible.

To further verify the feasibility and effectiveness of the designed controller, another desired trajectories are used as follows:

$$\begin{cases} y_1(t) = -50\sin(\pi t/150) + 50\sin(\pi t/10); \\ y_2(t) = 21\sin(\pi t/20) - 10\sin(\pi t/10); \\ y_3(t) = 30\cos(\pi t/40) + 52\cos(\pi t/10); \end{cases} \tag{97}$$

Then we obtain Fig. 6, from which, it can be seen that the helicopter can successful track the desired trajectory too.

According to the above simulation results, we can conclude that the helicopter can tracking the predefined trajectory within the acceptable range of error by using our proposed control.

5 Conclusion

In this paper, a RBFNN-based control method has been proposed to track arbitrary lateral, longitudinal and vertical reference trajectory in the presence of model uncertainties. The reference trajectory is planned for helicopter to avoid obstacles and collisions in known environment. Considering the unknown disturbances and uncertainties, the robust RBFNN-based controller has been investigated for the helicopter step by step. Finally, simulation results demonstrated that the helicopter is able to track the planned 3D spatial trajectory satisfactorily, with all other closed-loop signals bounded.

The presented method can also be extended to further trajectory tracking considering the posture of the helicopter in known or unknown environment. Furthermore, the proposed method can be extended by considering state, control and output constraints.

Acknowledgment This work was supported by the National Natural Science Foundation of China under Grant 61522302, the National Basic Research Program of China (973 Program) under Grant 2014CB744206, the project 973 (Grant No. 2014CB744904) Joint Founds of Civil Aviation and National

Natural Science (Grant No.U1533201), Civil aviation science and technology major projects (Project No. MHRD20130112), the Fundamental Research Funds for the Central Universities (Project No. 3122014C010), the Civil Aviation University of China (CAUC) Research Enabling Foundation under Grant 2015QD11S, and the Fundamental Research Funds for the China Central Universities of USTB under Grant FRF-TP-15-005C1..

References

1. Kandil, A.A., Wagner, A., Gotta, A., Badreddin, E.: Collision avoidance in a recursive nested behaviour control structure for unmanned aerial vehicles. In: 2010 IEEE International Conference on Systems, Man and Cybernetics, pp. 4276–4281. IEEE (2010)
2. Hoffer, N.V., Coopmans, C., Jensen, A.M., Chen, Y.: A survey and categorization of small low-cost unmanned aerial vehicle system identification. J. Intell. Robot. Syst. **74**(1-2), 129–145 (2014)
3. He, W., Zhang, S.: Control design for nonlinear flexible wings of a robotic aircraft. IEEE Trans. Control Syst. Technol. (2016). In Press, doi:10.1109/TCST.2016.2536708
4. Liu, H., Bai, Y., Lu, G., Shi, Z., Zhong, Y.: Robust tracking control of a quadrotor helicopter. J. Intell. Robot. Syst. **75**(3-4), 595–608 (2014)
5. Ge, S.S., Ren, B.B., Tee, K.P., Lee, T.H.: Approximation-based control of uncertain helicopter dynamics. IET Control Theory and Applications **3**(7), 941–956 (2009)
6. Sira-ramirez, H., Zribi, M., Ahmad, S.: Dynamical sliding mode control approach for vertical flight regulation in helicopters. In: IEEE Proceedings-Control Theory and Applications, vol. 141, pp. 19–24. IEEE (1994)
7. Yang, C.D., Liu, W.H., Kung, C.C.: Robust nonlinear H_∞ decoupling control of flight vehicle in hovering. In: IEEE Conference on Decision and Control, vol. 4, pp. 4486–4491. IEEE (2002)
8. Luo, C.C., Liu, R.F., Yang, C.D., Chang, Y.H.: Helicopter H_∞ control design with robust flying quality. Aerosp. Sci. Technol. **7**(2), 159–169 (2003)
9. Civita, M.L., Papageorgiou, G., Messner, W.C., Kanade, T.: Design and flight testing of an H_∞ controller for a robotic helicopter. J. Guid. Control. Dyn. **29**(2), 485–494 (2006)
10. Gadewadikar, J., Lewis, F., Subbarao, K., Chen, B.M.: Structured h-infinity command and control-loop design for unmanned helicopters. J. Guid. Control. Dyn. **31**(4), 1093–1102 (2008)
11. Johnson, E.N., Kannan, S.K.: Adaptive trajectory control for autonomous helicopters. J. Guid. Control. Dyn. **28**(3), 524–538 (2005)
12. Madani, T., Benallegure, A.: Backstepping control for a quadrotor helicopter. IEEE (2006)
13. Enns, R., Si, J.: Helicopter trimming and tracking control using direct neural dynamic programming. IEEE Transactions on Neural Network **14**(4), 929–939 (2003)
14. Cui, R., Ren, B., Ge, S.S.: Synchronised tracking control of multi-agent system with high order dynamics. IET Control Theory & Applications **6**(5), 603–614 (2012)
15. Chen, M., Ge, S.S., Ren, B.B.: Robust attitude control of helicopters with actuator dynamics using neural networks. IET Control Theory Applications **4**(12), 2837–2854 (2009)
16. Marconi, L., Naldi, R.: Robust full degree-of-freedom tracking control of a helicopter. Automatica **43**(11), 1909–1920 (2007)
17. Liu, D., Wang, D., Wang, F.-Y., Li, H., Yang, X.: Neural-network-based online HJB solution for optimal robust guaranteed cost control of continuous-time uncertain nonlinear systems. IEEE Transactions on Cybernetics **44**(12), 2834–2847 (2014)
18. Liu, D., Wang, D., Li, H.: Decentralized stabilization for a class of continuous-time nonlinear interconnected systems using online learning optimal control approach. IEEE Transactions on Neural Networks and Learning Systems **25**(2), 418–428 (2014)
19. Sun, C., Xia, Y.: An analysis of a neural dynamical approach to solving optimization problems. IEEE Trans. Autom. Control **54**(8), 1972–1977 (2009)
20. Liu, Z., Chen, C., Zhang, Y., Chen, C.L.P.: Adaptive neural control for dual-arm coordination of humanoid robot with unknown nonlinearities in output mechanism. IEEE Transactions on Cybernetics **45**(3), 521–532 (2015)
21. Liu, Z., Lai, G., Zhang, Y., Chen, X., Chen, C.L.P.: Adaptive neural control for a class of nonlinear time-varying delay systems with unknown hysteresis. IEEE Transactions on Neural Networks and Learning Systems **25**(12), 2129–2140 (2014)
22. Wei, H., Zhao, Y., Changyin, S.: "Adaptive Neural Network Control of a Marine Vessel with Constraints Using the Asymmetric Barrier Lyapunov Function". IEEE Transactions on Cybernetics. In Press, 2016 doi:10.1109/TCYB.2016.2554621
23. Wang, N., Er, M.J., Han, M.: Parsimonious extreme learning machine using recursive orthogonal least squares. IEEE Transactions on Neural Networks and Learning Systems **25**(10), 1828–1841 (2014)
24. Sun, C., He, W., Ge, W., Chang, C.: Adaptive Neural Network Control of Biped Robots. IEEE Transactions on Systems, Man, and Cybernetics: Systems (2016). In Press, 2016 doi:10.1109/TSMC.2016.2557223
25. Dai, S.-L., Wang, C., Wang, M.: Dynamic learning from adaptive neural network control of a class of nonaffine nonlinear systems. IEEE Transactions on Neural Networks and Learning Systems **25**(1), 111–123 (2014)
26. Wang, M., Wang, C.: Learning from adaptive neural dynamic surface control of strict-feedback systems. IEEE Transactions on Neural Networks and Learning Systems **26**(6), 1247–1259 (2012)
27. He, W., David, A.O., Yin, Z., Sun, C.: Neural network control of a robotic manipulator with input deadzone and output constraint. IEEE Trans. Syst. Man Cybern. Syst. (2016). In Press, doi:10.1109/TSMC.2015.2466194
28. Li, Z., Huang, Z., He, W., Su, C.-Y.: Adaptive impedance control for an upper limb robotic exoskeleton using biological signals. IEEE Trans. Ind. Electron. (2016). In Press, doi:10.1109/TIE.2016.2538741

29. Xu, B., Shi, Z., Yang, C., Sun, F.: Composite neural dynamic surface control of a class of uncertain nonlinear systems in strict-feedback form. IEEE Transactions on Cybernetics **44**(12), 2626–2634 (2014)
30. He, W., Dong, Y., Sun, C.: Adaptive neural impedance control of a robotic manipulator with input saturation. IEEE Trans. Syst. Man Cybern. Syst. **46**(3), 334–344 (2016)
31. Tee, K.P., Ge, S.S.: Control of nonlinear systems with partial state constraints using a barrier Lyapunov function. Int. J. Control., 2008–2023 (2011)
32. He, W., Ge, S.S., Li, Y., Chew, E., Ng, Y.S.: Neural network control of a rehabilitation robot by state and output feedback. J. Intell. Robot. Syst. **80**(1), 15–31 (2015)
33. Zhao, Z., He, W., Ge, S.S.: Adaptive neural network control of a fully actuated marine surface vessel with multiple output constraints. IEEE Trans. Control Syst. Technol. **22**(4), 1536–1543 (2014)
34. Liu, Y.-J., Chen, C.L.P., Wen, G., Tong, S.: Adaptive neural output feedback tracking control for a class of uncertain discrete-time nonlinear systems. IEEE Trans. Neural Netw. **22**(7), 1162–1167 (2011)
35. Lei, X., Ge, S.S., Fang, J.: Adaptive neural network control of small unmanned aerial rotorcraft. J. Intell. Robot. Syst. **75**(2), 331–341 (2014)
36. Cui, R., Yan, W.: Mutual synchronization of multiple robot manipulators with unknown dynamics. J. Intell. Robot. Syst. **68**(2), 105–119 (2012)
37. Li, Z., Ge, S.S., Adams, M., Wijesoma, W.: Robust adaptive control of uncertain force/motion constrained nonholonomic mobile manipulators. Automatica **44**(3), 776–784 (2008)
38. Li, Z., Yang, C., Tang, Y.: Decentralized adaptive fuzzy control of coordinated multiple mobile manipulators interacting with nonrigid environments. IET Control Theory & Application **7**(3), 397–410 (2013)
39. Li, Z., Huang, Z., He, W., Su, C.-Y.: Adaptive Impedance Control for an Upper Limb Robotic Exoskeleton Using Biological Signals. IEEE Transactions on Industrial Electronics. In Press, 2016, doi:10.1109/TIE.2016.2538741
40. Yang, C., Li, Z., Li, J.: Trajectory planning and optimized adaptive control for a class of wheeled inverted pendulum vehicle models. IEEE Transactions on Cybernetics **43**(1), 24–36 (2013)
41. Li, Z., Su, C.-Y.: Neural-adaptive control of single-master-multiple-slaves teleoperation for coordinated multiple mobile manipulators with time-varying communication delays and input uncertainties. IEEE Transactions on Neural Networks and Learning System **24**(9), 1400–1413 (2013)
42. Wu, H.-N., Wang, J.-W., Li, H.-X.: Design of distributed H_∞ fuzzy controllers with constraint for nonlinear hyperbolic PDE systems. Automatica **48**(10), 2535–2543 (2012)
43. Liu, Y.-J., Tong, S.: Adaptive fuzzy control for a class of nonlinear discrete-time systems with backlash. IEEE Trans. Fuzzy Syst. **22**(5), 1359–1365 (2014)
44. Li, H., Wu, C., Yin, S., Lam, H.: Observer-based fuzzy control for nonlinear networked systems under unmeasurable premise variables. IEEE Trans. Fuzzy Syst. (2016). doi:10.1109/TFUZZ.2015.2505331
45. Liu, Y.-J., Tong, S.: Adaptive fuzzy identification and control for a class of nonlinear pure-feedback MIMO systems with unknown dead zones. IEEE Trans. Fuzzy Syst. **23**(5), 1387–1398 (2015)
46. Wu, H.-N., Wang, J.-W., Li, H.-X.: Fuzzy boundary control design for a class of nonlinear parabolic distributed parameter systems. IEEE Trans. Fuzzy Syst. **22**(3), 642–652 (2014)
47. Li, H., Wang, L., Du, H., Boulkroune, A.: Adaptive fuzzy tracking control for strict-feedback systems with input delay and output constrain. IEEE Trans. Fuzzy Syst. (In Press)
48. Zhou, Q., Wang, L., Wu, C., Li, H., Du, H.: Adaptive fuzzy control for non-strict feedback systems with input saturation and output constraint. IEEE Trans. Syst. Man Cybern. Syst. (In Press)
49. Xiangpeng, X., Dong, Y., Huaguang, Z., Yusheng X.: Control Synthesis of Discrete-Time T-S Fuzzy Systems via a Multi-Instant Homogenous Polynomial Approach. IEEE Transactions on Cybernetics **46**(3), 630–640 (2016)
50. Xiangpeng, X., Dongsheng, Y., Hongjun, M.: Observer Design of Discrete-Time T-S Fuzzy Systems via Multi-Instant Homogenous Matrix Polynomials [J]. IEEE Transactions on Fuzzy Systems **22**(6), 1174–1179 (2014)
51. Kaixiang, P., Kai Z., Bo, Y., Jie, D., Zidong, W.: A quality-based nonlinear fault diagnosis framework focusing on industrial multimode batch processes. IEEE Transactions on Industrial Electronics, 2016 **64**(3), 2615–2624
52. Kaixiang, P., Kai, Z., Jie, D., Bo, Y.: Quality-relevant fault detection and diagnosis for hot strip mill process with multi-specification and multi-batch measurements. Journal of the Franklin Institute, 2015 **352**(3), 987–1006
53. Li, H., Gao, Y., Shi, P., Lam, H.-K.: Observer-based fault detection for nonlinear systems with sensor fault and limited communication capacity. IEEE Transactions on Automatic Control (2016). doi:10.1109/TAC.2015.2503566
54. O. L., et al.: Comparison of neural algorithms for function approximation. Pakistan Journal of Applied Sciences **2**, 288–294 (2002)
55. Padfield, G.: Helicopter flight dynamics: The theory and application of flying qualities and simulation modeling. AIAA, England (1996)
56. Isidori, A., Marconi, L., Serrani, A.: Robust nonlinear motion control of a helicopter. IEEE Trans. Autom. Control **48**, 413–426 (2003)
57. Koo, T., Sastry, S.: Differential flatness based full authority helicopter control design. In: Proceedings of the 38th IEEE Conference on Deision and Control, pp. 1982–1987. IEEE (1999)
58. Gavrilets, V.: Autonomous aerobatic maneuvering of miniature helicopters, Ph.D. dissertation, Massachusetts Institute of Technology (2003)
59. Tee, K.P., Ge, S.S.: Control of fully actuated ocean surface vessels using a class of feedforward approximators. IEEE Transactions on Control System Technology **14**(4), 750–760 (2006)
60. He, W., Ge, S.S., How, B.V.E., Choo, Y.S., Hong, K.-S.: Robust adaptive boundary control of a flexible marine riser with vessel dynamics. Automatica **47**(4), 722–732 (2011)

61. He, W., Zhang, S., Ge, S.S.: Robust adaptive control of a thruster assisted position mooring system. Automatica **50**(7), 1843–1851 (2014)
62. Chen, M., Ge, S.S., Ren, B.: Adaptive tracking control of uncertain mimo nonlinear systems with input constraints. Automatica **47**(3), 452–465 (2011)
63. He, W., He, X., Ge, S.S.: Vibration control of flexible marine riser systems with input saturation. IEEE/ASME Transactions on Mechatronics **21**(1), 254–265 (2016)
64. He, W., Ge, S.S.: Cooperative control of a nonuniform gantry crane with constrained tension. Automatica **66**(4), 146–154 (2016)
65. Liu, Y.-J., Tang, L., Tong, S., Chen, C.L.P., Li, D.-J.: Reinforcement learning design-based adaptive tracking control with less learning parameters for nonlinear discrete-time mimo systems. IEEE Transactions on Neural Networks and Learning Systems **26**(1), 165–176 (2015)
66. He, W., Ge, S.S.: Vibration control of a flexible beam with output constraint. IEEE Trans. Ind. Electron. **62**(8), 5023–5030 (2015)

Zhen Zhao received the B.Sc. degree in Automation from Northeastern University, Shenyang, China, in 2004 and the Ph.D. degree in Control Theory & Control Engineering from Northeastern University, Shenyang, China, in 2010. She worked as a Research Fellow in the Department of Electrical and Computer Engineering, National University of Singapore (NUS), Singapore, from 2011 to 2012. She is currently working as a Lecturer in the College of Electronics Information and Automation, Civil Aviation University of China, Tianjin 300300, China. Her current research interests include fault diagnosis and test for Avionics system.

Wei He received his B.Eng. degree from College of Automation Science and Engineering, South China University of Technology (SCUT), China, in 2006, and his PhD degree from Department of Electrical & Computer Engineering, the National University of Singapore (NUS), Singapore, in 2011. He worked as a Research Fellow in the Department of Electrical and Computer Engineering, NUS, Singapore, from 2011 to 2012. He is currently working as a full professor in School of Automation and Electrical Engineering, University of Science and Technology Beijing, Beijing, China. He has co-authored 1 book published in Springer and published over 100 international journal and conference papers. He is a Senior Member of IEEE. He serves as an Editor of Journal of Intelligent & Robotic Systems and IEEE/CAA Journal of Automatica Sinic. His current research interests include robotics, distributed parameter systems and intelligent control systems.

Zhao Yin received the B.Eng. degree in electric engineering and automation from Hangzhou Dianzi University, Zhejiang, China in 2013. He is currently working toward the M.E. degree in the School of Automation Engineering, University of Electronic Science and Technology of China, Chengdu, China. His current research interests include neural network control, adaptive control and robotics.

Jun Zhang received the B.Sc. and M.D degree in Physics from Northeastern University, Shenyang, China, in 2000 and 2007, and the Ph.D. degree in Logistics Scheduling and Optimization from Northeastern University, Shenyang, China, in 2014. He is currently working as a Lecturer in the College of Aerospace Engineering, Civil Aviation University of China, Tianjin 300300, China. His current research interests include logistics scheduling and optimization for airport and flight.